Experimental Study on a 4-b Serial Optical Digital to Analog Convertor

Tianhang Zhang
Qi Qiu
Zhiqiang Fan
Jun Su
Mingzhu Xu
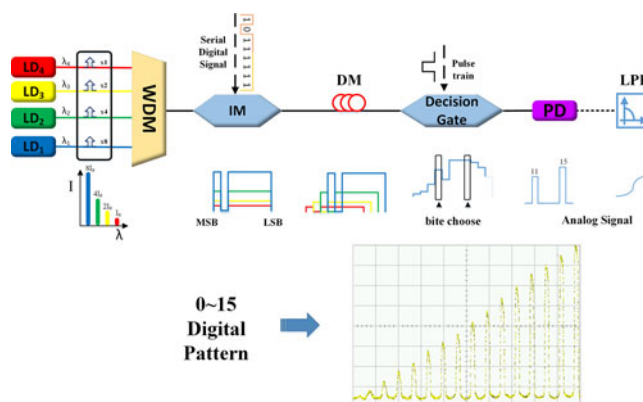
Experimental Study on a 4-b Serial Optical Digital to Analog Convertor

Tianhang Zhang ⓘ **, Qi Qiu** ⓘ **, Zhiqiang Fan** ⓘ **, Jun Su,**
and Mingzhu Xu ⓘ

School of Optoelectronic Information, University of Electronic Science and Technology of
China, Chengdu 610054, China

Abstract: Photonic techniques have potential to overcome the limitations of electronic digital-to-analog conversion. A serial optical DAC, using fiber dispersion with optical weighted wavelength multiplexing, is proposed and demonstrated. Serial Digital codes are overlapped regularly in time domain due to dispersion-based delays. Intensity information for the conversion is extracted by synchronous gating pulse train. The system is operated with a high precision time control. Performance of the ODAC is experimentally investigated by establishing a 4-b 12.5 Gb/s system. The linear transfer function is described and an ENOB of 3.55 is obtained. The proposed architecture could be easily modified for better performance.

Index Terms: Optical Digital-to-analog conversion, fiber dispersion, optic delay control.

1. Introduction

Digital-to-analog converter (DAC) and analog-to-digital converter are the key components in signal processing. They connect continuous signal in nature and discrete data in mathematical calculation. DACs are widely used in modern radars, arbitrary waveform generator and wireless communication, etc. The increasing requirement of digital signal processing for high speed and high precision can be satisfied with efficient DACs [1]. The conventional pure electronic approaches usually encounter the bottleneck in improving their frequency and bandwidth due to the inherent electronic limitation, such as RC delay, time jitter and electromagnetic interference. For current fabrication technologies and materials, there is a trade-off between conversion rate and bit resolution. To increase the speed and resolution at the same time, multiple electronic DACs are integrated into one system in different ways [2]. The performance is improved at the expense of system costs and complexity in this method. However, with the introduction of photonic techniques, the limitations of the electronic system can be circumvented. High-speed and large-bandwidth processing with the frequency of hundreds of gigahertz can be achieved [3]. Optical DAC (ODAC) is also compatible with fiber communication networks and free from the power consuming in electrical-optical conversion. Thus, the application of high-performance ODACs has been seen in in optical label switch, arbitrary waveform generator and visible light communication in recent years [4]–[6].

Changes of optical parameter, such as intensity, wavelength and phase, can be used to describe the conversion process. Weighting and summing of multi-channel optical intensity is a popular
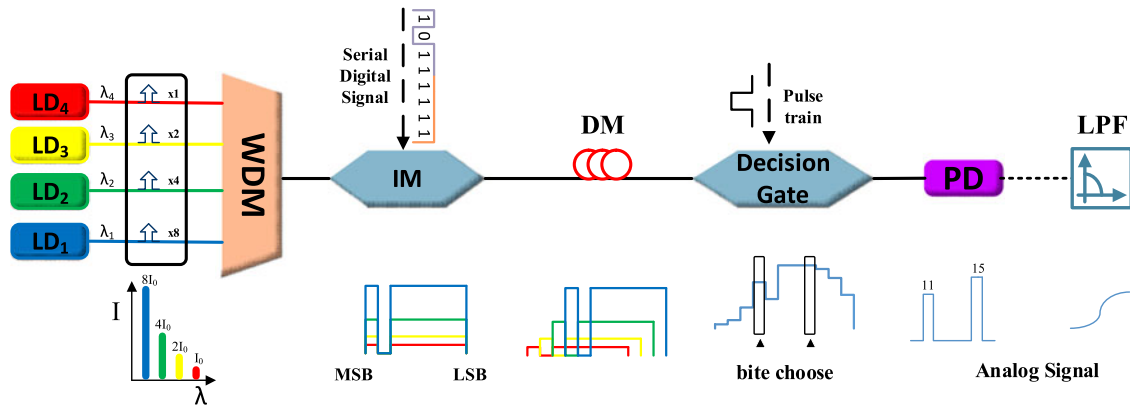
Fig. 1. Schematic diagram of the proposed ODAC illustrated by the example of 4-bit, the solid line represents optical link, the dash line represents electronic link, the waveform change is attached below. LD: laser diode; WDM: wavelength division multiplexer; IM: intensity modulator; DM: dispersive medium; PD: photo-detector; LPF: low pass filter; MSB: most significant bit; LSB: least significant bit.

method to implement an ODAC, and the structure is easy to realize as shown in [7]–[9]. Several kinds of ODACs are proposed, based on micro-ring resonators [10], nonlinear optical loop mirrors [11], polarization multiplexing [12] and phase shifters [13] are proposed. Besides, the bipolar ODAC with larger dynamic range can be realized by differential phase-shift keying (DPSK) modulation and balanced detection [14]. Those schemes were all designed for parallel digital signal mode, which can take full advantage of the speed superiority of photonic skills. And the bit resolution can be very high by accumulating parallel channels. However, most of the long-distance optical communication systems work in serial mode [15]. Additional serial-to-parallel conversion (SPC) is necessary for parallel ODACs to connect with optical communication systems. Moreover, the parameters synchronization of repetitive photonic devices used in parallel channels is the main cause that limits the system performance, especially for high bit resolution. Therefore, an increasing interest is focused on ODAC which can deal with serial digital signal. The relevant schemes were proposed for serial ODACs, which were based on temporal delay and summing [16], frequency generation by fiber nonlinear [17], spatial light modulation [18] and pulse pattern recognition [19]. Less number of devices is required in those kinds of schemes compared with parallel schemes. A single channel structure serial ODAC system was proposed and its improvement was achieved based on the chromatic dispersion and dispersion compensation of time and wavelength interleaved optical pulse train [20], [21]. Overcoming the disadvantages introduced by the imbalance of multiple channels, the system has better robustness than the previous one.

This paper, proposes a weighting and summing serial ODAC employing high-precision dispersion and time delay control. A detailed proof-of-principle experiment is conducted, and the performance of the system is investigated. Digital signal is transformed to multi-wavelength optical intensity weighted code stream and deformed by dispersion in a single fiber. A synchronized pulse work as decision gate extracts the desired information from the deformed waveform. The bit resolution of the system established is four and the bit rate is 12.5 Gbit/s. The system index such as linear transfer function and effective number of bits (ENOB) are investigated. Some kinds of waveforms generated by the experiment system are also displayed.

2. Operation Principle

The proposed schematic structure of the 4-bit serial ODAC is shown in Fig. 1. Four laser diodes (LD) and wavelength division multiplexer (WDM) are used to generate multi-wavelength continuous optical carrier with identical wavelength interval between adjacent wavelength components. By tuning the power of the laser sources, the optical components are intensity weighted to have a power

ratio of 8:4:2:1, where the shorter wavelength correspond to a higher intensity. The serial digital code stream with a bit rate of f bit/s is intensity modulated on the multi-wavelength carrier, where the least significant bit (LSB) is transmitted before the most significant bit (MSB). For electronic digital signal, electro-optic modulator (EOM) is adopted to accomplish the modulation. To deal with optical digital signal, wavelength conversion or all-optical modulation can be used [22], [23]. After modulation, the entire optical waveform S(t) of a 4-bit word start at time t can be described by

$$S(t_0) = \sum_{n=1}^{4} s_n(t_0) = \sum_{i=1}^{4} b_i \cdot P_{\Delta T}[t_0 + (i-1)\Delta T] \cdot \sum_{j=1}^{4} I_j \tag{1}$$

where $s_n(t)$ is the waveform of the component λ_n at time t, b_i is the digital code of i-th bit in a 4-bit word, $P_{\Delta T}(t)$ is a unit pulse starting at time t with pulse width ΔT, t_0 is the start time of the word, and I_j represents the optical intensity of different wavelength components, $I_1 = 2I_2 = 4I_3 = 8I_4 = 8I$.

Due to the anomalous chromatic dispersion in dispersive medium, an identical time delay is introduced between adjacent wavelength channels, while short-wavelength component travels faster. By properly setting the wavelength spacing and the length of dispersive medium, time delay ΔT equal to the width of the digital code can be achieved, as presented in (2).

$$\Delta T = D \cdot L_D \cdot \Delta\lambda \tag{2}$$

where D and L_D are dispersion coefficient and the length of the dispersive medium, respectively, $\Delta\lambda$ is the wavelength interval, where $\Delta\lambda = \lambda_2 - \lambda_1 = \lambda_3 - \lambda_2 = \lambda_4 - \lambda_3$. The waveform of the word is deformed to $S_D(t)$ because the different wavelength components are misplaced in time domain, as displayed in (3).

$$S_D(t_0) = \sum_{n=1}^{4} s_n[t_0 + (n-1)\Delta T] = \sum_{j=1}^{4}\sum_{i=1}^{4} b_i \cdot P_{\Delta T}[t_0 + (i-1)\Delta T + (j-1)\Delta T] \cdot I_j$$

$$= b_4 I \cdot P_{\Delta T}(t_0 + 6\Delta T) + (b_3 + 2b_4)I \cdot P_{\Delta T}(t_0 + 5\Delta T) + (b_2 + 2b_3 + 4b_4)I \cdot P_{\Delta T}(t_0 + 4\Delta T)$$

$$+ (b_1 + 2b_2 + 4b_3 + 8b_4)I \cdot P_{\Delta T}(t_0 + 3\Delta T) + (2b_1 + 4b_2 + 8b_3)I \cdot P_{\Delta T}(t_0 + 2\Delta T)$$

$$+ (4b_1 + 8b_2)I \cdot P_{\Delta T}(t_0 + \Delta T) + 8b_1 I \cdot P_{\Delta T}(t_0) \tag{3}$$

It can be seen that, the optical intensity of the 4-th bit (at time $t_0 + 3\Delta T$) in the waveform satisfies the binary algorithm of a 4-bit word. The deformed signal is on/off keying modulated by a Mach-Zehnder modulator (MZM) driven by consecutive gating pulse train with a repetition rate of f/4. The gating pulse width is no wider than the digital code. In this way, the right bits of each word with the intensity proportional to the weighted sum of digital code are picked out as in (4).

$$B_{\Delta T}(t) = S_D \cdot G_{\Delta T}[t_0 + 3\Delta T] = I \cdot R_G \cdot \sum_{n=1}^{4} b_n \cdot 2^{n-1} \tag{4}$$

where $G_{\Delta T}(t)$ is ΔT width gating pulse train starting at time t, R_G is the power coefficient of the gating pulse. The optical-to-electrical conversion is completed by a photo-detector (PD). The output power represents the amplitude of desired analog signal. An electrical low-pass filter (LPF) is used after PD to smooth the waveform.

In this scheme, the errors come from power fluctuation and temporal inaccuracy. The power fluctuation, which induce the output deviation from ideal value, is the sum of power errors from all wavelength components. The maximum value of output deviation is shown in (5).

$$E_{max} = \left[I \cdot \sum_{n=1}^{4} b_n \cdot \varepsilon_n \cdot 2^{n-1} \right]_{max} = (\varepsilon_1 + 2\varepsilon_2 + 4\varepsilon_3 + 8\varepsilon_4) \cdot I \tag{5}$$

where ε_n represents the power fluctuation percentage of each component. To guarantee the monotonicity of ODAC, E_{max} must be less than 1 LSB. According to the test methods given in the standard
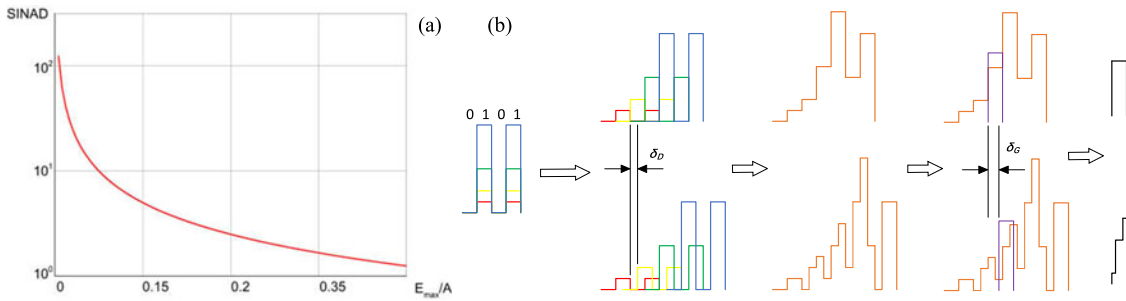
Fig. 2. (a) Relationship between SINAD and maximum power error; (b) the ideal waveform on the top and the waveform with time errors on the below.

[24], the signal to noise and distortion ratio (SINAD) and ENOB corresponding to maximum power error can be calculated by (6) and (7).

$$SINAD_{\min} = 20\log_{10}\left[\frac{A/\sqrt{2}}{\sqrt{\frac{1}{M}\sum_{n=1}^{M} E_{\max}^2}}\right] \tag{6}$$

$$ENOB_{\min} = \frac{SINAD - 10\lg 1.5}{20\lg 2} \tag{7}$$

where A is the amplitude of the signal, and M is the number of samples. The relationship between SINAD and maximum power error is shown in Fig. 2(a).

The temporal inaccuracy comprises gating mismatch and time delay errors caused by insufficient or excessive dispersion. All time errors can be regarded as inter symbol interference (ISI). Intensity value cannot be determined correctly because the powers from adjacent codes are mixed in the same time window. With time errors, (4) can be rewritten as (8).

$$B'_{\Delta T}(t_0) = G_{\Delta T}\left[t_0 + 3\Delta T + \delta_G\right] \cdot \sum_{n=1}^{4} s_n\left[t_0 + (n-1)\left(\Delta T + \delta_D\right)\right] \tag{8}$$

where δ_G represents gating pulse mismatch, and δ_D represents time delay errors. The effect of time errors on waveform change is shown in Fig. 2(b). As it can be seen, only part of intensity information of output time window is right, and the other part is submerged in adjacent codes. The wrong parts can be treated as power errors, which deteriorate the SINAD. Hence, the time accuracy is intolerable in this structure, and high-precision dispersion and time delay control are required.

The scheme proposed in this paper has advantages over previous systems in compacting system structure and can improve the conversion quality. The whole process of temporal changing and summing is completed in a single fiber. The devices used, such as intensity modulator, are all easy to be integrated. The errors caused by the mismatching between multiple channels, such as insert loss, and temperature difference, can be eliminated. Less intermediate process means fewer errors are introduced. Only the desired bit can pass through the choosing, which will make the output signal cleaner.

Besides, the bit resolution and the operation rate of the proposed system depend on the number of weighted light sources and the dispersion value of the fiber, respectively. It means that the system can be easily extended to get a higher bit resolution and higher speed. To realize higher bit resolution, more carries are required. One more bit means an extra carrier with shorter wavelength and the power is 3 dB higher than LSB, or with longer wavelength and power is 3 dB lower than MSB. The maximum power difference of an N-carriers system is 3(N − 1) dB, and the maximum wavelength difference is (N −1)$\Delta\lambda$. For example, the lowest power of eight unamplified laser diodes used in 8-bit system is 0 dBm, the highest power is up to 21 dBm. It can be achieved easily with
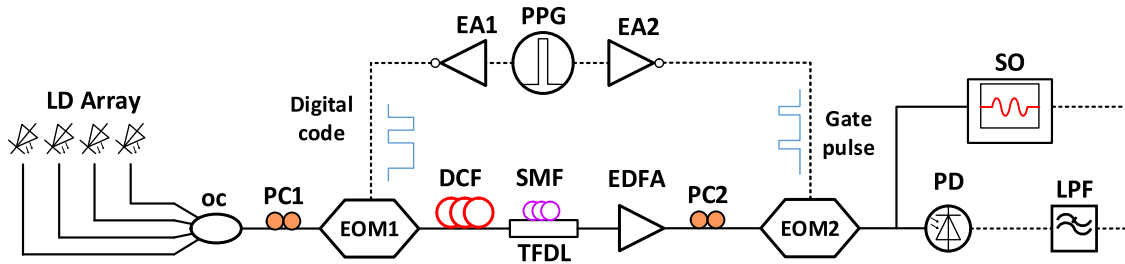
Fig. 3. Experiment setup of 4-bit ODAC, OC: optical coupler; PC: polarization controller; EA: electronic power amplifier; PPG: pulse pattern generator; DCF: dispersion compensation fiber; SMF: single mode fiber; TFDL: tunable fiber-optic delay line; SO: sampling oscilloscope.

commercial devices. The relationship between bit resolution and baud rate can be described by

$$R_{\text{baud}} = \frac{R_{bit}}{N} = \frac{1}{N} \cdot \frac{1}{\Delta T} = \frac{1}{D \cdot L_D \cdot \Delta\lambda \cdot N} \tag{9}$$

where R_{baud} represents baud rate, and R_{bit} represents bit rate. To improve baud rate and bit resolution at the same time, the length of dispersion compensation fiber should be modified or the wavelength interval is reduced. The improvement of the bit rate is limited by the performance of the modulation device and PD.

The next part, conducts an experiment on the proposed ODAC, and the performance is investigated in detail.

3. Experiment and Discussion

In the experiment, a 12.5 Gb/s 4-bit ODAC system is established as shown in Fig. 3. As mentioned before, the sampling rate and bit resolution are decided by the number of light source and the maximum bit rate of the pulse pattern generator (PPG), respectively. Four designed LDs and an optical coupler are used to generate the multi-wavelength carrier. Wavelength of those LDs are set to 1543.72 nm, 1546.92 nm, 1550.12 nm, and 1553.32 nm, with power set to 15 dBm, 12 dBm, 9 dBm, and 6 dBm, respectively. The stability of the light source is ± 0.25 dB/24 h, the fluctuation of input optical intensity can be ignored.

The intensity modulator (Oclaro Powerbit SD-20), driven by digital signal has a bandwidth larger than 20 GHz with an operation rate of up to 25 Gb/s and a half wave voltage of about 3.7 V @ 10 GHz. A 2-channel PPG (Anritsu MU181020A) with electronic power amplifiers is used to generate serial digital signal with a rate of 12.5 Gb/s and gating pulse train with a repetition rate of 3.125 GS/s. The dispersive medium is made up of a 170-meter dispersion compensation fiber (DCF) and a 57-meter single mode fiber (SMF) twined on a piezoelectric ceramic. The SMF part works as a tunable fiber-optic delay line (TFDL) to correct the time errors. Dispersion coefficient of the commercial DCF and SMF are -152.66 ps/(nm·km) and 16.7 ps/(nm·km) respectively. The dispersion is fine-tuned by precisely modifying the length of the SMF pigtail. The dispersion of whole special fiber is $-25 \pm 0.2-$ps/nm measured by differential phase-shift method. It means optical signal at adjacent wavelength is temporally separated by 80 ps with an error smaller than 1 ps.

Fifteen patterns from '0001' to '1111' are sent separately to test the dispersion, which are corresponding to 15 analog levels from '1' to '15'. The original electronic waveforms and the deformed optical waveforms after dispersion are shown in Fig. 4. As it can be seen, the intensity at the fourth bit of each optical waveform is proportional to the level of pattern.

Then, the deformed signal is cut by intensity modulator driven by gating pulse, which works as an optical switch. Temporal calibration is performed by tuning TDFL with the assistance of vector network analyzer (Anritsu 37369 D) to make sure gating pulse extracts the right time window. The result is detected by PD with a bandwidth of 20 GHz. The optical waveform after dispersion and
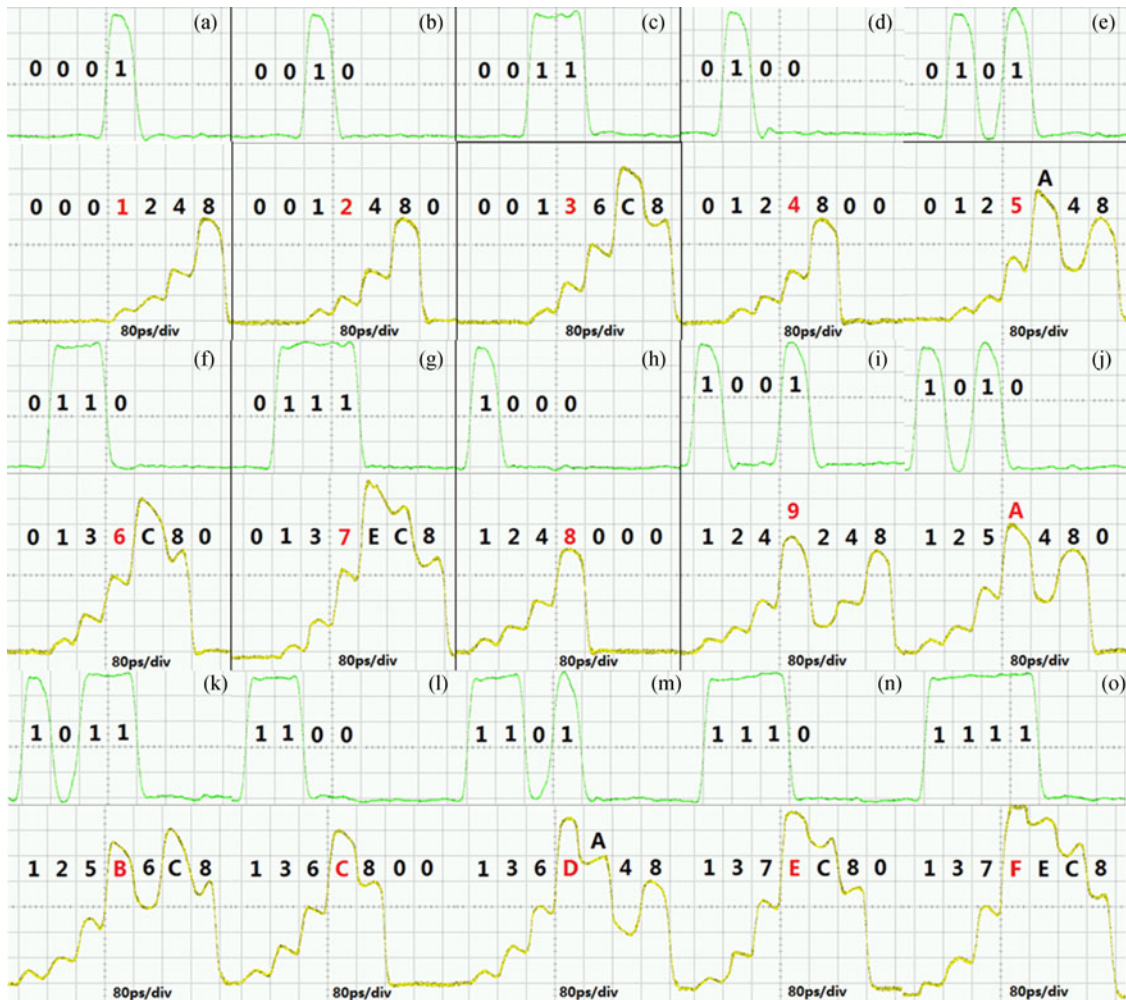
Fig. 4. The electronic waveform of the pattern from '0001' to '1111' and the optical waveform after dispersion. The green line represents electronic signal, the yellow line represents optical signal, with hexadecimal intensity label. The target bit is marked red.

the electronic waveform after low pass filtering are measured by a 90 GHz sampling oscilloscope (Agilent DCAX 86100D) with both electronic and optical receivers.

Consecutive code stream repeating periodically from pattern '0000' to '1111' is tested to investigate the performance of the ODAC. Due to the dispersion, each pattern overlaps with two adjacent patterns, and the newly mixed waveform is shown in Fig. 5(a). After being cut by gating pulse, an intensity-increased pulse train with temporal interval of 320 ps is presented in Fig. 5(b), which implies a sampling rate of 3.125 GS/s. The intensity of each pulse corresponding to the pattern input is measured to structure the transform function of the system in Fig. 6(a), and a linear fitting is attached also. With those measured data, the integral nonlinearity (INL) and differential nonlinearity (DNL) can be calculated, and the maximum value is 0.108 LSB and 0.479 LSB, respectively. The INL and DNL describe the deviation between the measured power and ideal one. Those power errors come from unequal insert loss between fours channels of the optical coupler, gain unflatness of EDFA for different wavelengths and the unstability of the electronic power amplifiers. It can be decreased using higher-performance devices.

There is no wrong code because of the high-precision dispersion and time delay control. The time calibration is performed to make sure the same phase of gating pulse train and optical signal.
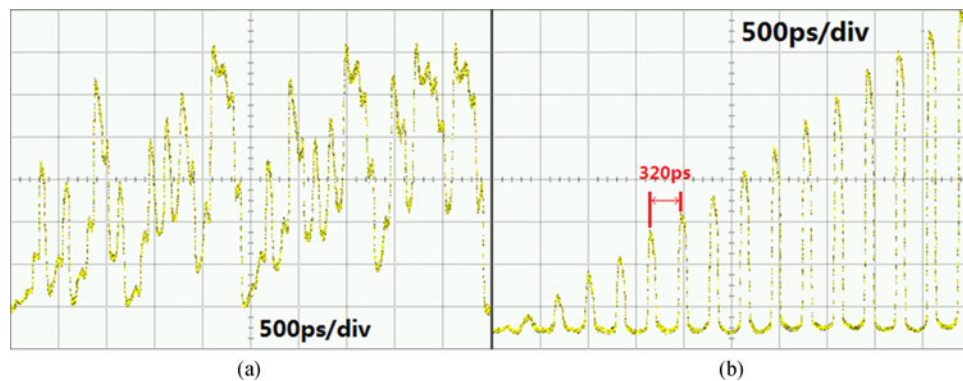
Fig. 5. Measured waveform of the optical pulses train for consecutive digital input from '0' to '15' after dispersion (a) and after bit choosing (b).
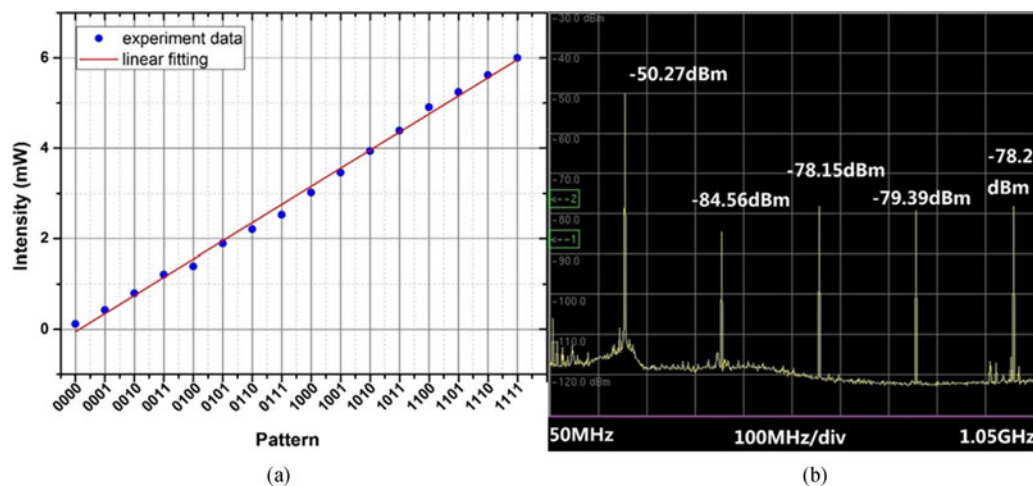

Fig. 6. (a) Measured optical pulse power and linear fitting, (b) Spectrum of the cosine waveform after LPF.

It indicates that the time difference should be integer times of 320 ps, which is the width of a 4-bit word. Calibration is operated by coarse tuning electronic delay and fine tuning optical delay. The electronic delay can be adjusted by changing the pattern of gating pulse train, with a step of 80 ps. The TFDL has an adjustable optical delay range of about 45 ps and the tuning step is hundreds femtosecond. So, the cutting deviation can be controlled within 1 ps. The length changing of TFDL stretched by piezoelectric ceramic is no more than 1 cm, which will not induce any error in dispersion. The ISI introduced by pulse broadening in fiber transmission can be ignored as the light source is narrow line-width and transmission distance is short. The total ISI can be controlled within a few picoseconds. And, for Gaussian type gating pulse with a full width at half maximum (FHWM) of 80 ps, most energy is concentrated on the middle part of the pulse. The ISI less than 5 ps on both edges can be suppressed. A gating pulse train with narrower pulse width can eliminate the errors introduced by ISI. However, narrower gating pulse width means more optical power is isolated, so the output signal power will be lower, which reduces the SINAD value.

In addition, the extinction ratio and modulation speed of modulator are the two main limitations of the proposed system. The intensity of the pattern '0000' is not absolute zero because the extinction ratio of EOM is just 20 dB, not high enough to cut off all optical power when driven by digital bit '0'. A modulator with an extinction ratio of about 20 dB can only make the bit resolution be less than
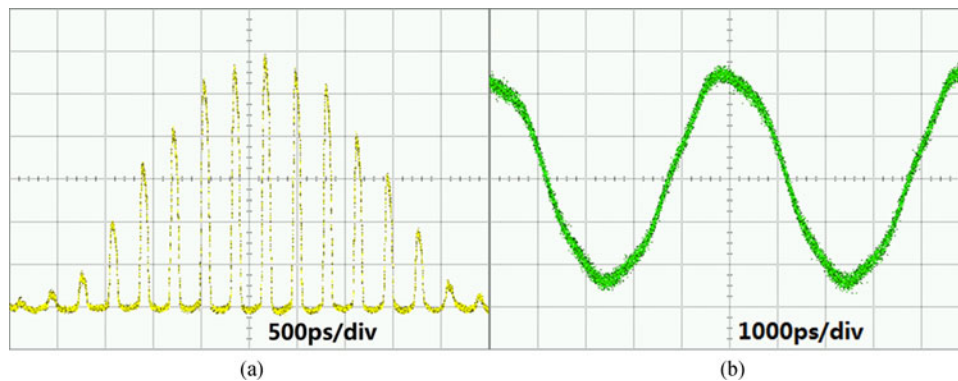
Fig. 7. (a) Cosine waveform consist of pulse train, (b) Cosine waveform after 980 MHz electronic LPF.
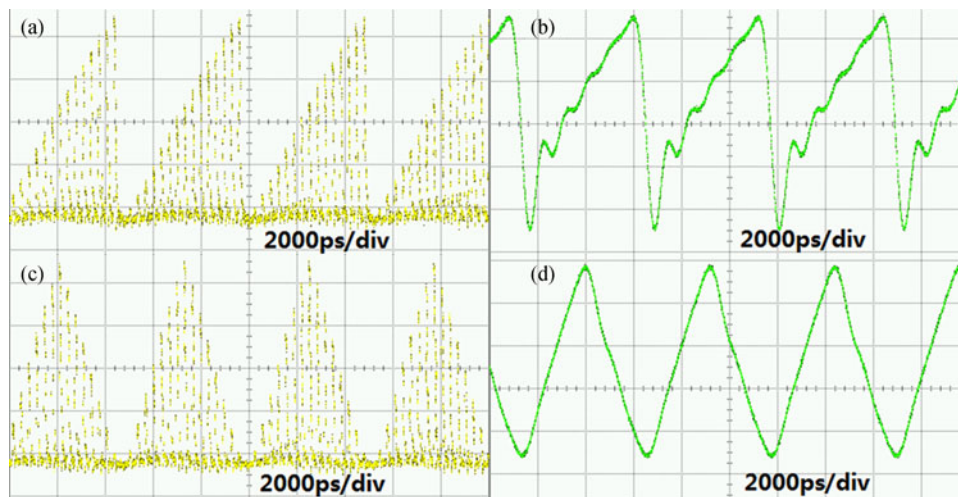

Fig. 8. (a) 195.3125 MHz triangular waveform consist of pulse train, (b) Triangular waveform after 980 MHz electronic LPF, (c) 195.3125 MHz saw-tooth waveform consist of pulse train, (d) Saw-tooth waveform after 980 MHz electronic LPF.

7 bits in theory. The commercial modulator with modulation speed more than 100 GHz can be used in the proposed to improve conversion speed. Furthermore, cross-gain modulation by semiconductor optical amplifiers may provide a new direction of improvement. It can reach high modulation speed with a good extinction ratio [25].

A cosine signal fitted by a designed 16-pulse sequence is generated to derive the ENOB of system. 64 bits are adopted to describe one signal cycle, which is corresponding to a signal frequency of 195.3125 MHz. Fig. 7 shows the waveform of cosine signal fitted by pulse train and the waveform after electronic LPF with a bandwidth of 980 MHz. The spectrum of the filtered cosine signal is obtained by a spectrum analyzer (Anritsu MS2725C) as shown in Fig. 6(b). Taking the second to fifth harmonics into calculation, the SINAD is 23.15 dB, and an ENOB of 3.55 can be derived.

A few kinds of waveforms are generated to evaluate the function of the ODAC as an arbitrary waveform generator. The results of triangular waveform and saw-tooth waveform are shown in Fig. 8. The same as the cosine waveform, a pulse train generated by the designed 64-bit digital code is used to fit the signal waveform in one cycle. Electronic LPF is used to smooth the waveform after PD. As it can be seen, the generated waveforms are close to the ideal one. Although the rising edge of triangular waveform is not as straight as expected because of the removal of high-frequency components after filtering, the performance of the proposed ODAC shows a good result.

4. Conclusion

A serial ODAC scheme based on the dispersion of weighted multi-wavelength carrier is proposed, and the performance is investigated. The digital signal is modulated on the carrier, and a dispersion process is introduced to mix each bit in time domain. A carving by gating pulse is followed to complete the digital-to-analog conversion. A designed dispersion fiber is used to realize high-precision dispersion control and to eliminate the phase deviation between the gating pulse and desired bit at the same time. In the experiment, the 4-bit ODAC system with a conversion speed of 12.5 Gb/s has a DNL of 0.108, an INL of 0.479 and an ENOB of 3.55. The proposed scheme has good potentials in extending for higher bit resolutions with higher operational speed.

References

[1] R. W Heath *et al.*, "An overview of signal processing techniques for millimeter wave MIMO systems," *IEEE J. Sel. Topics Signal Process.*, vol. 10, no. 3, pp. 436–453, Apr. 2016.

[2] C. Schmidta *et al.*, "High-speed digital-to-analog converter concepts," *Proc. SPIE*, vol. 10130, 2017, Art. no. 101300N.

[3] A. Bogoni *et al.*, "160 Gbit/s binary-to-quaternary amplitude shift keying encoding in the optical domain," *Opt. Lett.*, vol. 36, no. 11, pp. 1978–1980, 2011.

[4] K. Sawada and H. Uenohara, "High-speed optical label recognition technique using an optical digital-to-analog conversion and its application to optical label switch," *J. Lightw. Technol.*, vol. 28, no. 13, pp. 1889–1896, 2010.

[5] B. Gao, F. Zhang, and S. Pan, "Experimental demonstration of arbitrary waveform generation by a 4-bit photonic digital-to-analog converter," *Opt. Commun.*, vol. 383, pp. 191–196, 2017.

[6] J. Armstrong, "Optical domain digital-to-analog converter for visible light communications using LED arrays," *Photon. Res.*, vol. 1, no. 2, pp. 92–95, 2013.

[7] A. Yacoubian and P. K. Das, "Digital-to-analog conversion using electrooptic modulators," *IEEE Photon. Technol. Lett.*, vol. 15, no. 1, pp. 117–119, Jan. 2003.

[8] X. Yu *et al.*, "Incoherent photonic digital-to-analogue converter based on broadband optical source," *Electron. Lett.*, vol. 43, no. 19, pp. 1044–1045, 2007.

[9] J. Liao *et al.*, "Novel photonic radio-frequency arbitrary waveform generation based on photonic digital-to-analog conversion with pulse carving," in *CLEO: Science and Innovations*. Washington, DC, USA: Opt. Soc. Amer., 2015.

[10] L. Yang *et al.*, "Demonstration of a 3-bit optical digital-to-analog converter based on silicon microring resonators," *Opt. Lett.*, vol. 39, no. 19, pp. 5736–5739, 2014.

[11] S. Oda and A. Maruta, "All-optical digital-to-analog conversion using nonlinear optical loop mirrors," *IEEE Photon. Technol. Lett.*, vol. 18, no. 5, pp. 703–705, Mar. 2006.

[12] F. Zhang *et al.*, "Simplified 2-bit photonic digital-to-analog conversion unit based on polarization multiplexing," *Opt. Eng.*, vol. 55, no. 3, 2016, Art. no. 031115.

[13] A. Leven *et al.*, "High speed arbitrary waveform generation and processing using a photonic digital-to-analog converter," in *Proc. 2007 Digest IEEE/LEOS Summer Topical Meet.*, 2007, pp. 174–175.

[14] J. Liao *et al.*, "Novel bipolar photonic digital-to-analog conversion employing differential phase shift keying modulation and balanced detection," *IEEE Photon. Technol. Lett.*, vol. 25, no. 2, pp. 126–128, Jan. 2013.

[15] I. B. Djordjevic *et al.*, "Spatial-domain-based multidimensional modulation for multi-Tb/s serial optical transmission," *Opt. Exp.*, vol. 19.7, pp. 6845–6857, 2011.

[16] M. Gehl *et al.*, "2-Gb/s all-optical serial digital-to-analog converter," *Microw. Opt. Technol. Lett.*, vol. 51, no. 6, pp. 1561–1565, 2009.

[17] M. R. Chitgarha *et al.*, "Bit depth and sample rate tunable digital to analog converter using conversion/dispersion based delays," in *Proc. 2011 37th Eur. Conf. Exhib. Opt. Commun.*, 2011, pp. 1–3.

[18] F. Perennes, T. M. Coker, and W. A. Crossland, "Digital-to-analog image conversion with an optically addressed spatial light modulator," *Opt. Lett.*, vol. 22, no. 7, pp. 472–474, 1997.

[19] T. Nishitani *et al.*, "Demonstration and evaluation of all-optical digital-to-analog conversion using pulse pattern recognition based on optical correlation processing," in *Proc. Opt. Fiber Commun. Conf. Opt. Soc. Amer.*, 2006, Art. no. 10310.

[20] Y. Peng *et al.*, "Photonic digital-to-analog converter based on summing of serial weighted multiwavelength pulses," *IEEE Photon. Technol. Lett.*, vol. 20, no. 24, pp. 2135–2137, Dec. 2008.

[21] F. Zhang, B. Gao, and S. Pan, "Serial photonic digital-to-analog converter based on time and wavelength interleaving processing," in *Proc. 2016 25th IEEE Wireless Opt. Commun. Conf.*, 2016, pp. 1–4.

[22] A. Bazin *et al.*, "Ultrafast all-optical switching and error-free 10 Gbit/s wavelength conversion in hybrid InP-silicon on insulator nanocavities using surface quantum wells," *Appl. Phys. Lett.*, vol. 104, no. 1, 2014, Art. no. 011102.

[23] S. Yu *et al.*, "All-optical graphene modulator based on optical Kerr phase shift," *Optica*, vol. 3, no. 5, pp. 541–544, 2016.

[24] *IEEE Standard for Terminology and Test Methods of Digital-to-Analog Converter Devices*, IEEE Standard, 2012, pp. 1–126.

[25] O. Qasaimeh, "Cross-gain modulation in bistable quantum-dot VCSOAs," *IEEE Photon. Technol. Lett.*, vol. 29, no. 3, pp. 342–345, Feb. 2017.